Estimation of Kinetic Parameters based on Chirping Alfvén Eigenmodes

M. Lesur[1,2,3], Y. Idomura[1], K. Shinohara[4] and X. Garbet[2]

[1]Japan Atomic Energy Agency, Higashi-Ueno 6-9-3, Taitou, Tokyo. 110-0015, Japan
[2]Commissariat a l'Energie Atomique, Cadarache, 13108 StPaul-lez-Durance Cedex, France
[3]Ecole Doctorale de l'Ecole Polytechnique, 91128 Palaiseau Cedex, France
[4]Japan Atomic Energy Agency, Mukouyama 801-1, Naka, Ibaraki, 311-0193, Japan

E-mail: `maxime.lesur@polytechnique.org`

Abstract. Alfvén Eigenmodes (AEs) with frequency sweeping, or chirping AEs, are analyzed based on the so-called Berk-Breizman (BB) model. Kinetic parameter regimes with chirping nonlinear solutions are delimited in both supercritical and subcritical regimes. A new quasi-periodic chirping regime is found, and the quasi-period of chirping events depends on the linear growth rate. Based on these new findings, fundamental kinetic parameters such as the linear drive and the external damping rate are estimated by fitting nonlinear chirping characteristics between the experiment and the BB model. This approach is applied to Toroidicity-induced AEs on JT-60U, which suggests the existence of modes far from marginal stability. Two collision models are considered, and it is shown that dynamical friction and velocity-space diffusion are essential to reproduce nonlinear features observed in experiments. The results are validated by recovering measured growth and decay of perturbation amplitude, and by estimating collision frequencies from experimental equilibrium data.

1. Introduction

A major concern in burning plasmas is that high energy ions can excite plasma instabilities in the frequency range of AEs, which significantly enhance their transport. In general, the estimation of their mode growth rate γ is complex, and the question of their stability in ITER remains to be clarified. Linear theory predicts that the Toroidicity induced Alfvén Eigenmode [1] (TAE) is stable when the continuous damping of the background plasma exceeds the drive of fast particles. Thus, accurate estimations of fundamental kinetic parameters such as the linear drive γ_L and the damping rate γ_d are needed, especially if the system is close to marginal stability, where γ is sensitive to small variations of driving and damping terms. For this class of instabilities, the total growth rate can be estimated either by linear stability codes or by gyro- or drift-kinetic perturbative nonlinear initial value codes. This approach requires internal diagnostics, whose accuracy is not enough for robust estimations, and which are not always available. The global damping involves complicated mechanisms with details still under debate. Experimentally, γ_d can be estimated by active measurements of externally injected perturbations. However, the applicability of this technique is limited to dedicated experiments, and this prevents robust linear predictions of the stability of AEs.

Moreover, the existence of unstable AEs in a regime where linear theory predicts $\gamma < 0$, or subcritical AEs, has not been ruled out. To access the subcritical regime, nonlinear analysis is necessary.

This work is based on the following key point. Near the resonant surface, it is possible to obtain a new set of variables in which the three-dimensional plasma is described by a 1D Hamiltonian in two conjugated variables [2, 3, 4], if we assume an isolated single resonance. In this sense, the problem of AEs is homothetic to a simple 1D single mode bump-on-tail instability. The so-called Berk-Breizman (BB) problem [5, 2, 3, 6] is a generalization of the bump-on-tail problem, where we take into account an external wave damping accounting for background dissipative mechanisms at a rate γ_d, and a collision operator. Analogies between BB and AE physics enables more understanding of fully nonlinear problems in complex geometries by using a model that is analytically and numerically tractable, as a complementary approach to heavier 3D analysis.

Our analysis is limited to AEs with repetitive frequency sweeping of the resonant frequency, on a timescale much faster than the equilibrium evolution (chirping). Such behavior has been observed in the plasma core region of tokamaks JT-60U, DIII-D, START, MAST, NSTX, and in stellerators such as CHS. In most of the experiments, the frequency chirps by 10-30%, in a quasi-periodic fashion, with a period in the order of the millisecond.

In Sec. 2, we recall the equations of the BB model, and characterize the fully nonlinear behavior in the whole $(\gamma_d,\ \nu_a)$ parameter space, where ν_a is a Krook collision frequency, for a cold-bulk, weak warm-beam distribution. In addition to steady-state, periodic and chaotic regimes, which are delimited in Ref. [7], chirping and subcritical regions are delimited. In Sec. 3, we numerically investigate nonlinear chirping features. In some regimes, we found that chirping events present a quasi-periodic behavior. In Sec. 4, we apply BB theory to the TAE. Linear growth rates and collision frequencies for JT-60U TAE experiments are estimated by fitting nonlinear chirping characteristics.

2. The Berk-Breizman model

For the sake of concision, and to avoid numerical treatment of too large and too small numbers in simulations, we normalize time to the plasma frequency ω_p, distance to the Debye length λ_{D}, density to the initial total plasma density, and electric field to $q\lambda_{\mathrm{D}}/(mv_{th}^2)$, where $v_{th} = \lambda_{\mathrm{D}}\omega_p$, q and m are particle charge and mass, respectively.

We consider a 1D plasma with a distribution function $f(x, v, t)$. In the initial condition, the velocity distribution $f_0(v)$ comprises a cold Maxwellian bulk and a weak, warm beam of high-energy particles. The evolution of the distribution is given by the kinetic equation

$$\frac{\partial f}{\partial t} + v\,\frac{\partial f}{\partial x} + E\,\frac{\partial f}{\partial v} = \mathcal{C}(f - f_0), \tag{1}$$

where E is the electric field, and $\mathcal{C}(f - f_0)$ is a collision operator. In this work, we consider either Krook operator,

$$\mathcal{C}_{\mathcal{K}}(f - f_0) \; = \; -\nu_a(v)\,(f - f_0)\,, \tag{2}$$

and the one-dimensional projection of a Fokker-Plank operator [8], which includes a dynamical friction (drag) term and a velocity-space diffusion term,

$$\mathcal{C}_{\mathcal{FP}}(f - f_0) \; = \; \frac{\nu_f^2}{k}\frac{\partial\,(f - f_0)}{\partial v} \; + \; \frac{\nu_d^3}{k^2}\frac{\partial^2\,(f - f_0)}{\partial v^2}, \tag{3}$$

where k is the wave number for the resonance.

In the expression of the electric field,

$$E(x,t) \; = \; \hat{E}_k(t)e^{\imath kx} \; + \; c.c., \tag{4}$$

we assume a single mode of wave number k, reflecting the situation of an isolated single mode AE. The displacement current equation,

$$\frac{\partial E}{\partial t} \; = \; -4\pi \int v\,(f - f_0)\,\mathrm{d}v \; - \; 2\,\gamma_d\,E, \tag{5}$$

yields the time evolution of the wave. An external wave damping has been added to model all linear dissipation mechanisms of the wave energy to the background plasma that are not included in the previous equations [5]. In the collisionless limit, if we assume a small perturbation and a linear growth rate γ much smaller than the real frequency ω, linear calculations in the cold maxwellian limit yield the relation

$$\gamma \; = \; \gamma_L \; - \; \gamma_d, \tag{6}$$

where γ_L is the linear growth rate in the absence of external damping. In this limit, $\gamma_L = \gamma_{L0}$, where γ_{L0} is a measure of the slope of initial distribution at resonant velocity, $\gamma_{L0} \equiv (\pi\,\partial_v f_0|_{v=\omega/k})/(2k^2)$.

If the bulk particles interact adiabatically with the wave, their contribution to the Lagrangian can be expressed as part of the electric field. Then it is possible to adopt a perturbative approach, and to cast the BB model in a reduced form that describes the time evolution of the beam particles only [9, 10]. We refer to this reduced model as δf BB model. Compared to the full-f model, the δf model does not take into account effects of time-evolution of bulk particles, which is a caveat when assessing limit of theory that breaks-up when phase-space structures approach the bulk, but it has an advantage in the application to experiment, where we assume fixed mode structure, hence fixed background plasma.

The apparent simplicity of the equation system of the BB model hides surprisingly rich physics. In the unstable case, when the perturbation is small, linear theory predicts exponential growth of the wave amplitude. Then the trapping of resonant particles significantly modify the distribution function and an island structure appears. The saturation and following nonlinear evolutions are determined by a competition among the drive by resonant particles, the external damping, the particle relaxation which tends to recover the initial positive slope in the distribution function, and particle trapping that tends to smooth it. Four kinds of behaviors emerge, namely steady-state, periodic, chaotic, and chirping responses, depending on the strength of each factor.

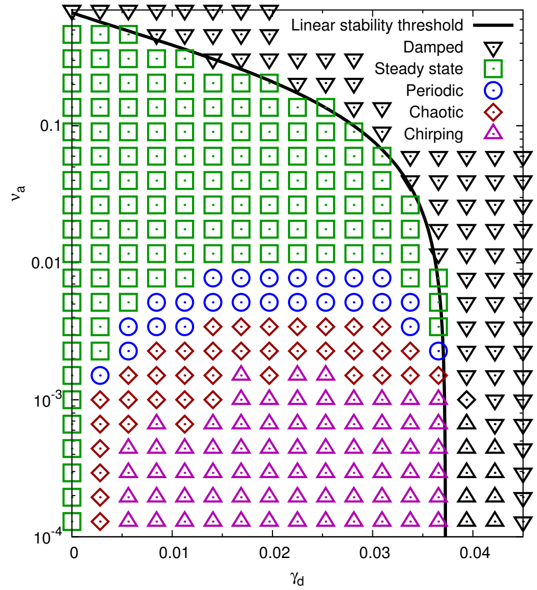

Figure 1. Behavior bifurcation diagram for a cold bulk, weak warm beam distribution. The classification of each solution is plotted in the $(\gamma_d,\ \nu_a)$ parameter space. The solid curve is the linear stability threshold obtained by solving the linear dispersion relation numerically. Diamonds and triangles on the right of the linear stability threshold, which are not included in the legend, represent subcritical instabilities.

In Ref. [11], we developed kinetic codes capable of long-time simulations of δf and full-f BB model in various parameter regimes. We refer to these codes as δf COBBLES and full-f COBBLES, respectively, COBBLES standing for COnservative Berk-Breizman semi-Lagrangian Extended Solver. We perform a series of full-f COBBLES simulations with Krook collisions, in the whole $(\gamma_d,\ \nu_a)$ parameter space. The initial bump-on-tail distribution parameters are chosen such that we stay within the validity limit of BB theory, with a cold bulk and a weak warm beam. The characterization of the behavior of the wave amplitude obtained in our simulations is shown in Fig. 1.

Note the agreement between linear stability threshold and the boundary between linearly stable and unstable simulations. For small collision rates, we observe instabilities in the linearly stable region, which suggests the possibility of subcritical instabilities.

3. Nonlinear features of chirping

Chirping solutions arise in a low collision regime when hole and clump structures [2] are formed in phase-space. They belong to a chaotic regime, and each chirping event is slightly different. In this work, we are interested in the nonlinear chirping characteristics, averaged over a significant number of chirping events.

In Ref. [12], the time-evolution of the frequency shift is obtained, in the collisionless limit, as

$$\delta\omega(t) \ = \ \alpha\, \gamma_{L0}\, \sqrt{\gamma_d\, t}, \tag{7}$$

with $\alpha \approx 0.44$. These analytic expressions have been found to agree with 1D simulations of both δf and full-f BB model, [11, 12], with both Krook and diffusion-only collision operators. In Sec. 4, we consider a regime with relatively fast sweeping, $\dot{\delta\omega}/\omega_b^2 \approx 0.5$, where $\omega_b \equiv (k|E_k|)^{1/2}$ is the bounce frequency. In this regime, it is necessary to introduce the effect of non-adiabaticity on chirping velocity as a correction parameter β, defined as

$$\beta \equiv \frac{\delta\omega(t)}{\alpha\,\gamma_{L0}\,\sqrt{\gamma_d\,t}}. \tag{8}$$

A numerical investigation confirms that β approaches unity in a regime of adiabatic hole/clump evolution. Even for relatively large values of $\dot{\delta\omega}/\omega_b^2$, the chirping velocity has a smooth dependency on the kinetic parameters [13]. The latter point is crucial for the validity of the procedure described in Sec. 4.

The resonant velocity of a hole (a clump) does not increase (decrease) indefinitely. We define the life-time τ of a chirping event as the time in which the corresponding power in the spectrogram decays below a fraction e^{-2} of the maximum amplitude that is reached during this chirping event. The maximum life-time $\tau_{\max}$ reached by τ during a time-series, ignoring the first chirping event and any minor event, follows

$$\tau_{\max} = \frac{\iota_a}{\nu_a}, \tag{9}$$

in the Krook case, where ι_a is a constant, which we evaluate by fitting numerical simulations, as $\iota_a = 1.1$. In the case with drag and diffusion, $\tau_{\max}$ scales like

$$\tau_{\max} \sim \frac{\gamma_{L0}^2}{\nu_d^3}, \tag{10}$$

when $\nu_f \ll \nu_d$, only for low collisionality. For higher collisionality, diffusion affects the width of a hole or clump during the first phase of their evolution, namely drive by free-energy extraction, which in turn affects the decay by diffusion. Since chirping observed in experiments belongs to this regime, we adopt a semi-empirical law obtained by a linear fit of numerically obtained life-time,

$$\tau_{\max} = \iota_d \left(\frac{\gamma_{L0}^2}{\nu_d^3}\right)^{0.5}, \tag{11}$$

with $\iota_d = 10$.

As long as the background plasma parameters are not significantly changed, chirping events in most tokamak experiments are quasi-periodic, with a quiescent phase between two chirping branches that lasts a few milliseconds. In some parameter regimes, chirping arising from the BB model with Krook collisions is also quasi-periodic, although the phase between two major chirping events is generally not as quiet as in the experiments. In a regime where $\nu_f \ll \nu_d$, chirping arising from the BB model with drag and diffusive collisions is quasi-periodic too, but this time with clear quiescent phases in-between chirping events. In both case, no analytic theory has been developed to predict the average time between two chirping events, Δt_{chirp}. However, conceptually, there exists some relation with a subset of the input parameters. Thus, if we normalize time with the mode frequency, then chirping velocity, life-time and period are dictated

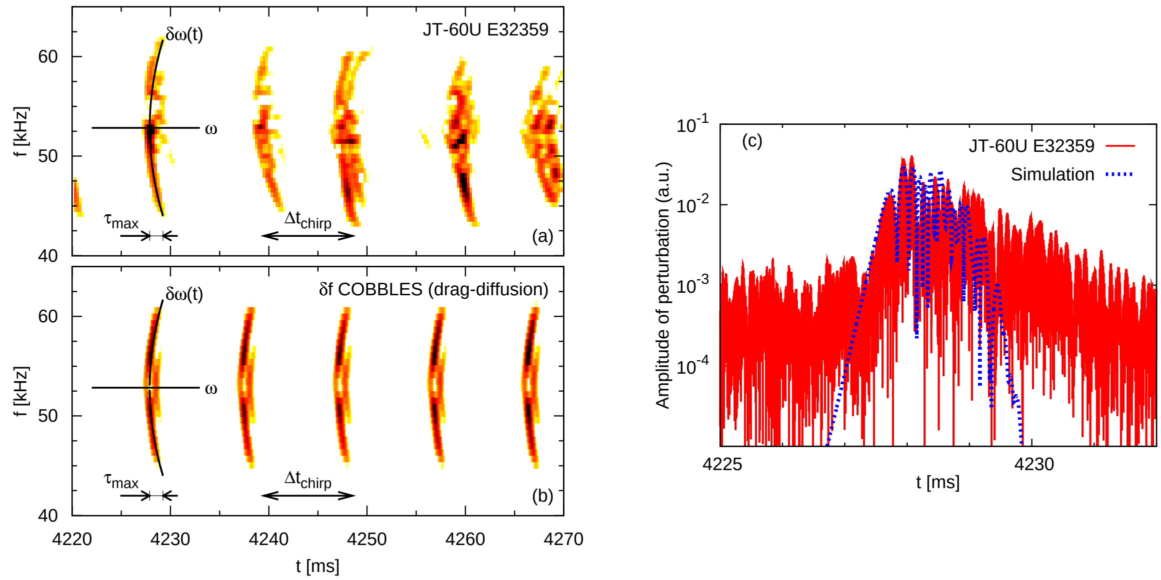

Figure 2. (a) Spectrogram of magnetic fluctuations during fast-FS modes in the JT-60U discharge E32359. (b) Spectrogram of the electric field, where the kinetic parameters of the δf BB model with friction-diffusion collisions were chosen to fit (a). Solid curve shows the analytic prediction for the chirping velocity. (c) Evolution of the amplitude of perturbations during a single chirping event. The signal is filtered between 40 and 65 kHz. In these arbitrary units, 10^{-3} roughly corresponds to a noise level.

by the input parameters of the model, γ_{L0}, γ_d, and ν_a, or ν_f and ν_d. With drag and diffusion, we have a 4-variables, 3-equations system, hence the solution is not unique, but the boundaries of chirping regime limit the possible range of input parameters.

4. Spectroscopic analysis of chirping TAEs on JT-60U

In JT-60U, TAEs are destabilized by a negative ion based neutral beam (N-NB), which injects deuterons at 360 keV. A distinction is made between so-called abrupt large-amplitude events (ALE) and fast frequency sweeping (fast-FS) [14]. Here, we focus on the latter phenomenon, which has a timescale of $1 - 5$ ms. In the discharge E32359, around $t = 4.2$ s, quasi-periodic, perturbative chirping frequency sweeping modes are observed. They have been identified as $m/n = 2/1$ and $3/1$ TAEs [15]. In the spectrogram, which is shown in Fig. 2(a), we measure a mode frequency $f_{\mathrm{A}} = 53$ kHz, to which we re-normalize time in our simulations. We also measure the average chirping velocity $d\delta\omega^2/dt = 6.3 \times 10^{-5}$, the maximum chirping life-time $\tau_{\max} = 0.44 \times 10^3$, and the average chirping period $\Delta t_{chirp} = 3 \times 10^3$ (on average).

The analysis described here aims at estimating the values of γ_{L0}, γ_d, ν_f and ν_d for which the δf BB model fits experimental observations. The comparison is possible if we consider a time interval where background plasma parameters are not significantly changed, since a fixed mode structure is assumed to reduce the problem to a one dimensional Hamiltonian. We also assume that frequency shifting occurs well within the gap of the Alfvén continuum, so that chirping lifetime is determined by collision processes, rather than by continuum damping. Here we focus on collision operators with drag and diffusion, since an attempt to fit experiments within the framework of Krook collisions yielded unconvincing results.

Eqs. (8) and (11) give two relations between linear drive, external damping, and velocity-diffusion coefficient. On the one hand, it is shown in Ref. [8] that for typical NBI-heated experiments, the ratio ν_d/ν_f is of the order of unity. On the other hand, a numerical exploration of chirping regimes with drag and diffusion suggests that when $\nu_f \geq \nu_d$, the drag significantly modifies the shape of chirping, to the point where we leave the regime of repetitive chirping. Thus the relevant regime for friction is $\nu_f \lesssim \nu_d$. In this regime, Δt_{chirp} increases with decreasing ν_f, γ, and increasing ν_d. Our fitting procedure consists of a 2D scan in $(\nu_f,\, \nu_d)$, where we search for solutions that fit the chirping period. If the experiment belongs to a regime where $\beta = 1$, the above procedure is systematic. In general, $\beta \neq 1$, and trial-and-errors are required to adjust chirping velocity to the experimental value.

We perform a first, rough scan, assuming $\beta = 1$. Measuring average chirping velocity in repetitive chirping solutions yields an estimation of the correction parameter, $\beta = 0.75$. We perform a second, more careful scan, which consists of a series of 4×8 simulations in the domain $(0.015 \leq \nu_d \leq 0.022,\ 1 \leq \nu_d/\nu_f \leq 8)$, where γ_{L0} and γ_d are constrained by Eqs. (8) and (11). The only repetitive chirping solution with $2500 < \Delta t_{chirp} < 3500$ we found is shown in Fig. 2(b). We verify that chirping features measured in this simulation, $d\delta\omega^2/dt = 7.1 \times 10^{-5}$ (6.2×10^{-5} for up-chirping, 7.9×10^{-5} for down-chirping), $\tau_{\max} = 0.45 \times 10^2$ (0.47×10^2 for up-chirping, 0.43×10^2 for down-chirping), and $\Delta t_{chirp} = 3.1 \times 10^3$, fit the experiment. The estimated linear parameters, in percentage of $\omega_{\mathrm{A}} = 2\pi f_{\mathrm{A}}$, are $\gamma_{L0} = 9.8\%$, $\gamma_L = 8.8\%$, $\gamma_d = 4.7\%$, $\nu_f = 0.36\%$, $\nu_d = 1.7\%$, and $\gamma = 4.6\%$. In theory, the solution is not unique, but the latter estimation is quite accurate because of the narrow range of periodic chirping regime. To validate this analysis, we compare the amplitude of perturbations in Fig. 2 (c). Since the growth rate of chirping structure is neither γ nor γ_L, and the decay rate not simply γ_d, but a function of several linear parameters, the agreement we obtain is not trivial (We measure a growth rate of 2.3%, and a decay rate of 0.3%).

For further validation, we estimate the values of ν_f and ν_d, by projecting a Fokker-Planck collision operator on the resonant surface [8]. This procedure yields $\nu_f = 1.2\%$ and $\nu_d = 1.7\%$. Note that electrons account for 99% of ν_f^2, which reflects a high Alfvén velocity, while impurities account for 57% of ν_d^3, which is consistent with the fact that pitch-angle scattering is more effective with heavier particles. We find a quantitative agreement for ν_d. However, with our fitting procedure, ν_f was underestimated by 70%. Though error bars in the experimental data may account for this discrepancy, it is also possible that our model misses some mechanism that would enhance the friction.

5. Conclusion

We delimited a chirping regime in both supercritical and subcritical regions. We showed that chirping velocity agrees with theory in a regime of adiabatic hole/clump evolution. In a low collisionality limit, the chirping life-time scales like analytic predictions, and we gave a semi-empirical law that fits life-time measured in simulations for experimental-level collisions.

We showed that the BB model can successfully reproduce features observed in the experiment if the collision operator includes drag and diffusion terms. In this case, we find a good agreement between simulation and measured growth and decay of perturbation amplitude. The velocity-diffusion coefficient obtained with our fitting procedure quantitatively agrees with an estimation from experimental equilibrium measurements. Note that major advantages of our fitting technique are 1. kinetic parameters in the core of the plasma estimated only from the spectrogram of the magnetic fluctuations measured at the edge, without expensive MHD calculations nor detailed core diagnostics, and 2. unified treatments of supercritical and subcritical AEs.

Acknowledgments

The main author thanks Y. Todo, P. Diamond, F. Zonca, S. Pinches, C. Nguyen and N. Dubuit for fruitful discussions. This work was performed within the frame of a co-thesis agreement between the doctoral school of the Ecole Polytechnique, the Japan Atomic Energy Agency, and the Commissariat à l'Energie Atomique. It was supported by both the JAEA Foreign Researcher Inviting Program and the European Communities under the contract of Association between EURATOM and CEA, and by the MEXT, Grant No. 22866086. Travel expenses for the IAEA-NFC 2010 conference were kindly provided by NFRI-WCI. The views and opinions expressed herein do not necessarily reflect those of the European Commission. Computations were performed on Altix3700 and BX900 systems at JAEA, and on Norma system at CEA.

[1] Cheng C Z, Chen L and Chance M S 1985 *Annals of Physics* **161** 21–47 URL `http://dx.doi.org/10.1016/0003-4916(85)90335-5`
[2] Berk H L, Breizman B N and Pekker M S 1997 *Plasma Physics Reports* **23** 778–788 URL `http://adsabs.harvard.edu/abs/1997PlPhR..23..778B`
[3] Breizman B N, Berk H L, Pekker M S, Porcelli F, Stupakov G V and Wong K L 1997 *Phys. Plasmas* **4** 1559–1568 URL `http://link.aip.org/link/?PHP/4/1559/1`
[4] Wong H V and Berk H L 1998 *Phys. Plasmas* **5** 2781–2796 URL `http://link.aip.org/link/?PHP/5/2781/1`
[5] Breizman B N, Berk H L and Ye H 1993 *Phys. Fluids B* **5** 3217–3225 URL `http://pop.aip.org/pfbpei/v5/i9/p3217-s1`
[6] Berk H L, Breizman B N and Pekker M 1996 *Phys. Rev. Lett.* **76** 1256–1259
[7] Vann R G L, Dendy R O, Rowlands G, Arber T D and d'Ambrumenil N 2003 *Phys. Plasmas* **10** 623–630 URL `http://link.aip.org/link/?PHP/10/623/1`
[8] Lilley M K, Breizman B N and Sharapov S E 2009 *Phys. Rev. Lett.* **102** 195003
[9] Berk H L, Breizman B N and Pekker M 1995 *Phys. Plasmas* **2** 3007–3016 URL `http://link.aip.org/link/?PHP/2/3007/1`
[10] Cary J R and Doxas I 1993 *J. Comput. Phys.* **107** 98–104 ISSN 0021-9991
[11] Lesur M, Idomura Y and Garbet X 2009 *Phys. Plasmas* **16** 092305–+
[12] Berk H L, Breizman B N and Petviashvili N V 1997 *Phys. Lett. A* **234** 213–218
[13] Lesur M, Idomura Y, Shinohara K, Garbet X and the JT-60 Team 2010 *Phys. Plasmas* To appear
[14] Shinohara K, Kusama Y, Takechi M, Morioka A, Ishikawa M, Oyama N, Tobita K, Ozeki T, Takeji S, Moriyama S, Fujita T, Oikawa T, Suzuki T, Nishitani T, Kondoh T, Lee S, Kuriyama M, JT-60 Team, Kramer G J, Gorelenkov N N, Nazikian R, Cheng C Z, Fu G Y and Fukuyama A 2001 *Nucl. Fusion* **41** 603–612
[15] Kusama Y, Kramer G J, Kimura H, Saigusa M, Ozeki T, Tobita K, Oikawa T, Shinohara K, Kondoh T, Moriyama M, Tchernychev F V, Nemoto M, Morioka A, Iwase M, Isei N, Fujita T, Takeji S, Kuriyama M, Nazikian R, Fu G Y, Hill K W and Cheng C Z 1999 *Nucl. Fusion* **39** 1837–1843